Sensors and Actuators B 209 (2015) 258–264

Contents lists available at ScienceDirect

Sensors and Actuators B: Chemical

journal homepage: www.elsevier.com/locate/snb

Colorimetric and fluorometric detection of anionic surfactants with water soluble sensors

Yingyuan Zhao [b], Xiyou Li [a,b,*]

[a] Xinjiang Technical Institute of Physics and Chemistry, CAS, Urumqi, China
[b] Key Laboratory of Colloid and Interface Chemistry, Ministry of Education, Department of Chemistry, Shandong University, China

ARTICLE INFO

Article history:
Received 19 October 2014
Received in revised form
21 November 2014
Accepted 25 November 2014
Available online 2 December 2014

Keywords:
Anionic surfactant
Fluorescence spectrum
Absorption spectrum
Naphthalimide
Probe

ABSTRACT

Five amphiphilic naphthalimide derivatives were synthesized and applied as colorimetric and fluorometric probes for the detection of anionic surfactants. Because of electrostatic and hydrophobic interactions, the probe and anionic surfactant can form complex in water. The formation of the probe–anionic surfactant complex induces distinctive changes on color and optical properties. Therefore, these derivatives can be used as sensors for anionic surfactants. Besides the advantage of visual detection, the detection of anionic surfactant can be realized by both absorption and fluorescence methods with high selectivity and sensitivity.

1. Introduction

Because of their highly potent detergency and low cost of manufacture, anionic surfactants are used in greater volume than any other surfactants in the detergent industry [1–3]. Hence anionic surfactants are becoming one of the major components of environmental pollutants. Apart from the efforts in studying methods to reduce their environmental impact, another important aspect is the development of new and improved detecting methods in environment.

Although many well-known techniques in surfactant analysis, including methylene blue method [4], ion-selective electrodes capillary electrophoresis method [5], and so forth [6], have been developed, there exist still some limitations in their applicability, such as tedious procedures, large amount of toxic solvents, irreproducibility, signal instability, temperature and pH sensitivity [7–10]. Therefore, it is still attractive to find new simple and sensitive approaches for in site anionic surfactant detection.

An and co-workers developed an anionic surfactant detection method based on the disassembly of the complex between a cationic conjugated polyelectrolyte (CPE), poly(3-(4-methyl-3′-thienyloxy)propyltrimethylammonium (PMTPA) and an anionic dye, 8-hydroxy-1,3,6-pyrenetrisulfonic acid risodium salt (HPTS) [11]. Coll and co-workers used hybrid systems for colorimetric signaling of anionic surfactants in water [12,13]. Chen and co-workers developed an imidazolium-based conjugated polydiacetylene sensor for colorimetric and fluorescent detection of anionic surfactants [14]. These methods mentioned above are all based on supramolecular interactions of anionic surfactants with conjugated polymers. The difficulty on the synthesis and quality control of the polymers is the main drawback for these methods. Qian and co-workers reported a series of relatively simple molecular “on–off–on” fluorescent sensors for detecting anionic surfactants based on the electrostatic and hydrophobic interactions between sensors and anionic surfactants [15]. However, the solubility of these molecular sensors in water is small, therefore, polar non-protonic solvents, such as DMF, must be employed in the sensing process. For the purpose of simplifying the sensing process and avoiding the use of expensive and poison solvents, water soluble fluorescent probes are most desired.

Herein, five naphthalimide-based cationic dyes (**1a**, **1b**, **1c**, **2b** and **3b** shown in Chart 1) were designed and synthesized for the purpose of applying as probes for the detection of anionic surfactants with both absorbance and fluorescence changes. The cationic hydrophilic headgroups endow the sensors with a strong electrostatic interaction with anionic surfactant. Meanwhile, the n-alkyl hydrophobic chains endow these dyes with a comparatively

* Corresponding author at: Key Laboratory of Colloid and Interface Chemistry, Ministry of Education, Department of Chemistry, Shandong University, China. Tel.: +86 0531 88369877; fax: +86 0531 88564464.
E-mail address: xiyouli@sdu.edu.cn (X. Li).

http://dx.doi.org/10.1016/j.snb.2014.11.122
0925-4005/

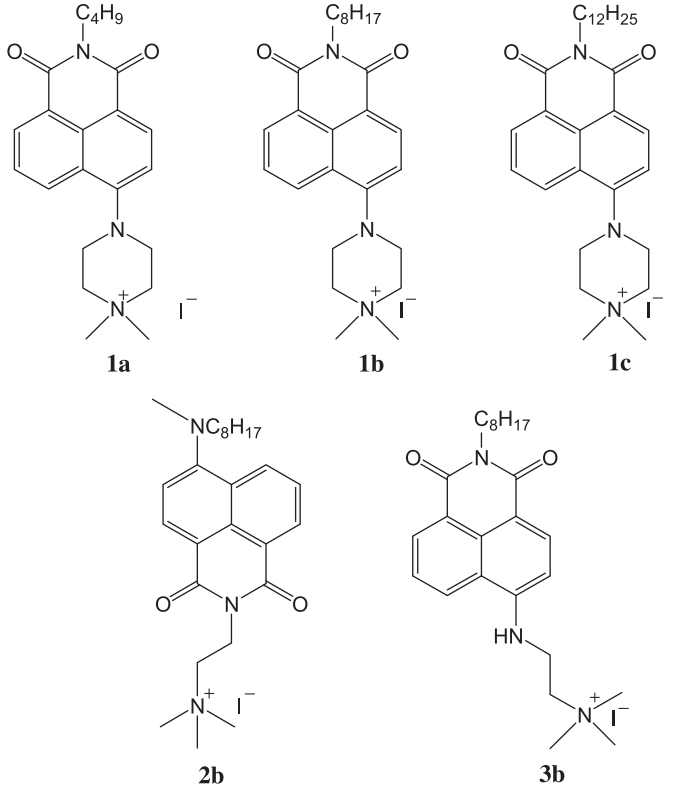

Chart 1. Molecular structures of the probes.

strong hydrophobic interaction with anionic surfactants. A stable complexes of dye-anionic surfactant based on static attraction is expected. Accordingly, the spectroscopic properties of the probes will change significantly in the presence of anionic surfactants and thus successfully achieve the sensing of anionic surfactants.

2. Experimental

2.1. Reagents

Sodium dodecylsulfate (SDS, 99%) was obtained from Alfa Aesar, while sodium dodecylsulfonate (SDSO, 99%) was bought from J&K. Sodium dodecylbenzenesulfonate (SDBS, 95%), sodium dodecanoate (SD, 98%) and hexadecyltrimethylammonium bromide (CTAB, 99%) were purchased from Aladdin. Triton X-100 (TX-100 AR) was bought from Sinopharm Chemical Reagent Co., Ltd. Pluronic P123 (AR) was a product of Sigma. Triply distilled water was used as solvent throughout the experiments. All other chemicals are of analytical grade and were purchased from commercial source and used as received without further purification.

2.2. Synthesis

1a, **1b**, **1c** were synthesized according to the procedure reported in our previous work [16]. The synthetic procedures of **2b** and **3b** are presented in Supporting Information. All the products were characterized by ^{1}H NMR and mass spectrometry (MS).

1a ^{1}H NMR ($CDCl_3$): δ 8.24 (m, 3H, H_{naph}), 7.63 (t, J = 10.0 Hz, 1H, H_{naph}), 7.28 (d, J = 10.0 Hz, 1H, H_{naph}), 3.88 (t, J = 8.1 Hz, 2H, C_3CH_2N), 3.75 (t, J = 6.6 Hz, 4H, $NaphNCH_2CH_2$), 3.57 (t, J = 5.2 Hz, 4H $(CNCH_2CN)_2$), 3.28 (s, 6H, CH_3NCH_3), 1.52 (m, 2H, C_2CH_2C), 1.30 (m, 2H, CCH_2C_2), 0.86 (t, J = 8.0 Hz, 3H, CH_3C_3). ESI–MS (Q-TOF): calcd. for $C_{22}H_{28}N_3O_2$: 366.2176; found: 366.2122 (M^+).

1b ^{1}H NMR ($CDCl_3$): δ 8.55 (d, J = 8.2 Hz, 1H, H_{naph}), 8.50 (d, J = 9.0 Hz 1H, H_{naph}), 8.45 (d, J = 9.1 Hz, 1H, H_{naph}), 7.77 (t, J = 9.1 Hz, 1H, H_{naph}), 7.41 (d, J = 8.1 Hz, 1H, H_{naph}), 4.16 (m, 2H, C_7CH_2N), 4.11 (s, 4H, $NaphNCH_2CH_2$), 3.76 (s, 6H, CH_3NCH_3), 3.62 (s, 4H $(CNCH_2CN)_2$), 1.70 (m, 2H, C_6CH_2C), 1.38 (m, 10H, $(CH_2)_5$), 0.86 (t, J = 8.0 Hz, 3H, CH_3C_7). ESI–MS (Q-TOF): calcd. for $C_{26}H_{36}N_3O_2$: 422.2808; found: 422.2769 (M^+).

1c ^{1}H NMR ($CDCl_3$): δ 8.55 (d, J = 8.2 Hz, 1H, H_{naph}), 8.50 (d, J = 8.2 Hz, 1H, H_{naph}), 8.45 (d, J = 9.0 Hz,1H, H_{naph}), 7.76 (t, J = 9.1 Hz,1H, H_{naph}), 7.40 (d, J = 9.0 Hz, 1H, H_{naph}), 4.15 (t, J = 7.9 Hz, 2H, $C_{11}CH_2N$), 4.11 (s, 4H, $NaphNCH_2CH_2$), 3.73 (s, 6H, CH_3NCH_3), 3.60 (s, 4H, $(CNCH_2CN)_2$), 1.70 (m, 2H, $C_{10}CH_2C$), 1.25 (m, 18H, $(CH_2)_9$), 0.87 (t, J = 7.6 Hz, 3H, CH_3C_{11}). ESI–MS (Q-TOF): calcd. for $C_{30}H_{44}N_3O_2$: 478.3434; found: 478.3450 (M^+).

2b ^{1}H NMR ($CDCl_3$): δ 8.58 (d, J = 7.5 Hz, 1H, H_{naph}), 8.46 (m, 2H, H_{naph}), 7.68 (t, J = 8.0 Hz, 1H, H_{naph}), 7.14 (d, J = 9.2 Hz, 1H, H_{naph}), 4.66 (t, J = 7.3 Hz, 2H, NCH_2CNCO), 3.90 (t, J = 7.1 Hz, 2H, $NCCH_2NCO$), 3.60 (s, 9H, $(CH_3)_3N$), 3.38 (t, J = 8.0 Hz, 2H, $CNCH_2C_7$), 3.11 (s, 3H, CH_3NC_8), 1.74 (m, 2H, CCH_2C_6), 1.29 (m, 10H, $(CH_2)_5$), 0.87 (t, J = 7.8 Hz, 3H, CH_3C_7). ESI–MS (Q-TOF): calcd. for $C_{26}H_{38}N_3O_2$: 424.2958; found: 424.3062 (M^+).

3b ^{1}H NMR ($CDCl_3$): δ 8.74 (d, J = 10.1 Hz, 1H, H_{naph}), 8.44 (d, J = 8.1 Hz, 1H, H_{naph}), 8.28 (d, J = 10.2 Hz 1H, H_{naph}), 7.57 (t, J = 9.2 Hz 1H, H_{naph}), 6.58 (d, J = 9.2 Hz 1H, H_{naph}), 4.17 (s, 4H, NCH_2CH_2N), 4.07 (t, J = 7.1 Hz, 3H, C_7CH_2), 3.55 (s, 9H, $(CH_3)_3N$), 1.65 (m, 2H, C_6CH_2C), 1.28 (m, 10H, $(CH_2)_5$), 0.86 (t, J = 7.2 Hz 3H, CH_3C_7). ESI–MS (Q-TOF): calcd. for $C_{26}H_{38}N_3O_2$: 410.2802; found: 410.2811 (M^+).

2.3. Apparatus

Electronic absorption spectra were recorded on a UV-2450 spectrophotometer (SHIMADZU, Japan). The steady-state fluorescence measurements were carried out on a FLS920 fluorescence spectrometer (Edinburgh Instruments). ESI–MS were measured on Q-TOF LC/MS 6510 (Agilent). ^{1}H NMR spectra were recorded on a Bruker 300 MHz NMR spectrometer with the solvent peak as internal standard (in $CDCl_3$).

3. Results and discussion

3.1. Optical properties of the dyes

The photophysical properties of 1,8-naphthalimide compounds are governed by the nature of the substituent [17]. Connection of electron donating groups at C-4 position of the naphthalic ring gives a "push–pull" electronic configuration and generate an internal charge transfer (ICT) excited state [18,19]. The five dyes investigated in this article are all quaternary ammonium salt and the presence of positive charge center (N^+) could influence the dipolemoment and then affect their optical properties, such as the wavelength of the maximal absorption and emission bands (λ_{max}) and the fluorescence quantum yield. This has been successfully demonstrated by the comparison of the absorption and emission spectra of **1b** with that of **5b**, a compound without quaternary ammonium headgroup, as shown in Fig. 1. The spectra revealed that the presence of N^+ leads to a remarkable blue-shift on ICT absorption and emission band. Simultaneously, the fluorescence quantum yield of **1b** is much greater than that of **5b**. These can be attributed to the strong electron withdrawing ability of N^+, which induces a "pull–push–pull" electronic configuration [20–23], But in **5b**, due to the absence of N^+, the photoinduced electron transfer from the amino group to the naphthalic ring gets efficient and the fluorescence is quenched significantly.

The fluorescence properties of these five dyes in H_2O and CH_2Cl_2 at the concentration of 1×10^{-5} M are summarized in Table 1. The fluorescence quantum yields of these five dyes are also measured

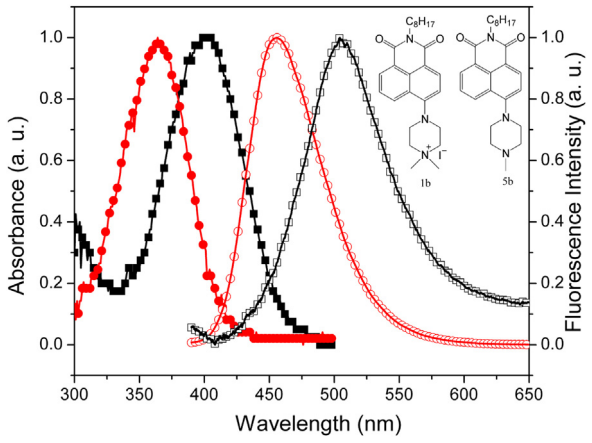

Fig. 1. Normalized absorption (solid) and fluorescence (hollow) spectra of **1b** (circle) and **5b** (square) in CH_2Cl_2. Inset shows the molecular structures of **1b** and **5b**.

with rhodamine 6G in ethanol (95%) as reference [24–26]. It is obvious that the difference on the length of hydrophobic chains does not obviously influence λ_{max} of the absorption and emission spectra of **1a**, **1b**, and **1c**. However, along with the increase on the length of hydrophobic chains, the fluorescence quantum yields decrease obviously, following the order of **1a** > **1b** > **1c** in H_2O, but **1c** > **1b** > **1a** in CH_2Cl_2. The difference on the hydrophobic chain length causes different solubility in solvent, therefore, the changes of fluorescence quantum yields can be attributed to the different solubility of these three dyes in H_2O and CH_2Cl_2. Relatively poor solubility induces more aggregation in solution, which causes more fluorescence quenching, and consequently reduce the fluorescence quantum yield.

Comparing with compound **1b**, compound **3b** presents red-shifted λ_{max} in absorption and emission spectra as well as a smaller Stoke's shift. These can be attributed to the flexible linkage between the ammonium cation (N^+) and the N at C-4 position in **3b**, which leads to a relative larger distance between N^+ and N, and then a weaker effect of N^+ on the "pull–push–pull" electronic configuration of NDI. The ICT characteristic of the excited state is enforced a little, therefore, the maximum absorption and emission wavelength are red-shifted.

As for compound **2b**, the N^+ is connected at the opposite position of the electron donating part, which provides a "push–pull–pull" electronic configuration for the molecules of this compound, therefore, the ICT characteristic of the excited states of this compound is further enforced in comparison with that of **3b**. So the λ_{max} of the absorption and emission spectra of compound **2b** are the most red-shifted and the fluorescence quantum yield is the smallest among these five compounds.

The steady state absorption and fluorescence spectra of these five compounds as discussed above suggest that the absorption and emission λ_{max} and the fluorescence quantum yields of these compounds can be tuned efficiently in a large range by changing the position of the electron-withdrawing N^+ on the NDI ring. This provides us an opportunity to design and synthesis of new NDI dyes to meet the needs of different applications.

3.2. Detection of SDS by *1b*

Because the presence of N^+ and long hydrophobic chain in these 1,8-naphthalimide-based molecules, the optical properties of these compounds become sensitive to the surrounding environment. This provides us the opportunity to use these molecules as probes to detect anionic surfactants in solution.

As shown in Fig. 2, upon addition of SDS into the aqueous solution of **1b** (1×10^{-5} M), the maximal absorption and emission bands were blue-shifted from 387 to 370 nm and 525 to 496 nm, respectively, indicating the presence of strong interactions between SDS and **1b**. The addition of SDS in **1b** aqueous solution leads to a regular decrease in the absorption intensity and fluorescence quenching first. The intensity of the absorption and fluorescence band reaches a minimum value at a SDS concentration of ~0.01 mM, suggesting a 1:1 stoichiometry for the complex SDS–**1b**. When SDS concentration is higher than 0.01 mM, both the absorption and fluorescence intensities were recovered and finally exceeded their initial values. Therefore, **1b** is an "on–off–on" fluorescence probe for anionic surfactant SDS. The dynamic detection window of SDS was 1×10^{-7} M–1×10^{-5} M and the detection limit of SDS was 1×10^{-7} M (28.7 ppb) with **1b** as probe.

The strong electrostatic and hydrophobic interactions between **1b** and SDS are believed to be responsible for the formation of SDS-**1b** complexes [27]. The phase behavior of the cationic–anionic surfactant system can be transformed along with the change of cationic/anionic surfactant molar ratio [28]. Generally, when the ratio between the cationic and the anionic surfactants is exactly 1:1, a precipitate could be formed [29]. But, due to the very small concentrations of both **1b** and SDS (smaller than 1×10^{-5} M), the formed SDS-**1b** cannot precipitate from solution, but formed large aggregates instead, therefore, we cannot observe any precipitate in the solution. Owing to the formation of large aggregates, the absorbance and fluorescence intensity decreased progressively. Moreover, the photoinduced electron transfer from the negatively charged head group of SDS to the fluorophore might be another reason for the quenching of the fluorescence of the dye [15]. When the concentration of SDS is higher than 0.01 mM, along with the increase of SDS concentrations, the value of SDS/**1b** will be much larger than 1, therefore, SDS-**1b** precipitates will be dissociated gradually [15], leading to the decrease on the number and size of the aggregates. Thus, the absorbance and fluorescence were recovered.

The shifts on the wavelength of the maximal absorption and emission bands are related to the different composition of SDS-**1b** complex. Along with the increase of the SDS molecules around **1b**, the maximal absorption and emission bands blue-shifts gradually because of the smaller polar condition provided by the SDS molecules with respect to water molecules. To further prove this point, temperature dependent absorption and fluorescence spectra of **1b** in SDS solution were measured (Fig. S1) because intermolecular aggregation is sensitive to temperature [30] and the SDS-**1b**

Table 1
Fluorescence properties of the dyes.

Compound	H_2O				CH_2Cl_2			
	λ_{abs} (nm)	λ_{em} (nm)	Φ_f (%)[a]	Stokes shift	λ_{abs} (nm)	λ_{em} (nm)	Φ_f (%)[a]	Stokes shift
1a	387	525	32.78	138	365	456	24.63	91
1b	387	525	23.81	138	365	456	25.37	91
1c	387	525	16.77	138	365	456	31.86	91
2b	457	533	0.62	76	443	527	17.45	84
3b	429	526	18.01	97	412	475	19.58	63

[a] With rhodamine 6G in ethanol (Φ_f = 95%) as standard.

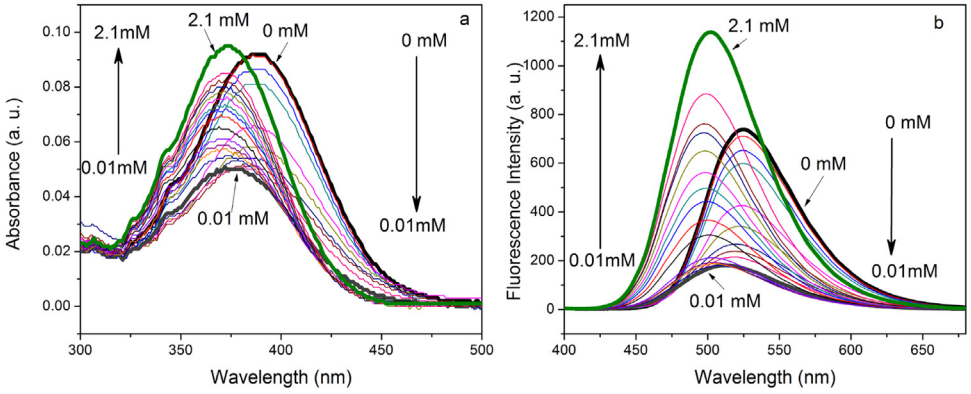

Fig. 2. (a) Effects of the concentration of SDS on the absorption spectra of **1b** in aqueous solution at 25 °C. (b) Effects of the concentration of SDS on the fluorescence spectra of **1b** in aqueous solution at 25 °C.

complex might be broken at elevated temperatures. The results are shown in Fig. S1 in Supporting Information. It revealed clearly that along with the increase of temperature, the maximal absorption and emission bands were red-shifted gradually and the intensity decreased first and then recovered to or excess its original intensity, signifying the SDS-**1b** complexes were being dissociated gradually. As shown in Scheme 1, the dissociation is a two-step process. Step 1 is the escape of SDS molecules and the reformation of SDS-**1b** aggregates, therefore, the optical intensities decrease first. Step 2 is the dissociation of SDS-**1b** aggregates.

Notably, there exists a good linear relationship between fluorescence quantum yield of **1b** and the concentration of SDS. Fig. 3a shows the relationship between the fluorescence quantum yield of **1b** and the concentration of SDS from 1×10^{-7} M to 6×10^{-6} M ($R = 0.9790$), which shows a "turn-off" response. A better linear relationship between the fluorescence quantum yield and the concentration of SDS from 5×10^{-5} to 1.9×10^{-3} mM ($R = 0.9993$) with good reproducibility is shown in Fig. 3b. This implies that **1b** is potentially useful for the quantitative determination of SDS concentrations, especially for SDS concentrations in the range of 5×10^{-5}–1.9×10^{-3} mM. Because **1b** shows a "turn-on" response in this concentration range, which is very sensitive due to the extremely low background noise and high quantum yield of **1b** [11]. The changes of **1b** absorbance could also be used to quantitatively detect the concentration of SDS, however, the detection range is relatively narrow (Fig. S2).

In addition to the quantitative determination by fluorescence quantum yield, qualitative determination of SDS could be achieved by measuring the shifts of the maximal absorption and emission bands with respect to that of **1b** in pure water ($\Delta\lambda_{abs} = \lambda_{0abs} - \lambda_{abs}$, where λ_{0abs} refers to the wavelength of the absorption band of **1b** in pure water and λ_{abs} refers to the wavelength of the absorption band of **1b** in SDS solutions, $\Delta\lambda_{em} = \lambda_{0em} - \lambda_{em}$, where λ_{0em} refers to the wavelength of the emission band of **1b** in pure water and λ_{em} refers to the wavelength of the emission band of **1b** in SDS solutions) along with the concentration increase of SDS. As shown in Fig. 4a, when SDS concentrations are lower than 3×10^{-6} M, $\Delta\lambda_{abs}$ keeps constant. Beyond this concentration (3×10^{-6} M), $\Delta\lambda_{abs}$ increases progressively to another constant, 17 nm. The change of $\Delta\lambda_{em}$ is similar with that of $\Delta\lambda_{abs}$. According to $\Delta\lambda_{abs}$ and $\Delta\lambda_{em}$, the detection limit of SDS is 3×10^{-6} M (0.86 ppm). Simultaneously, a dramatic color change from light-yellow to colorless was observed along with the increase of SDS concentration, which can be identified easily by naked eyes, Fig. S4.

3.3. The influence of probe structures

To investigate the effects of the molecular structure of the probe on the formation of SDS-probe complexes, the photophysical properties of **1a**, **1c**, **2b** and **3b** were investigated in the presence of different concentration of SDS. Along with the increase of SDS concentration, the maximal absorption and fluorescence bands of **1a**, **1c**, **2b** and **3b** were all blue shifted, which is similar to those of **1b** (Fig. S3 in the supporting information), indicating the presence of strong interactions between these molecules and SDS. These blue shifts may be attributed to the increase of the SDS molecules around

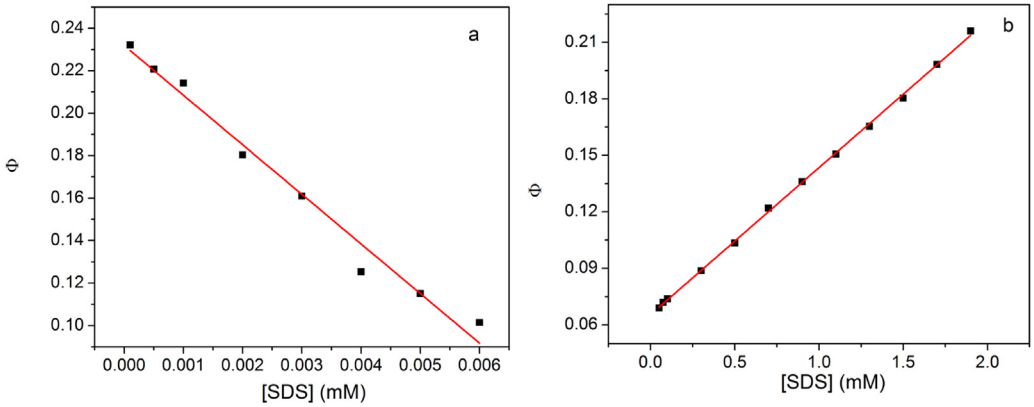

Fig. 3. (a) The relationship between the fluorescence quantum yield of **1b** and the concentration of SDS from 0.0001 to 0.006 mM. $R = 0.9790$. (b) The relationship between the fluorescence quantum yield of **1b** and the concentration of SDS from 0.05 to 1.9 mM. $R = 0.9993$. The fluorescence quantum yields are calculated with rhodamine 6G in ethanol ($\Phi_f = 0.95$) as standard.

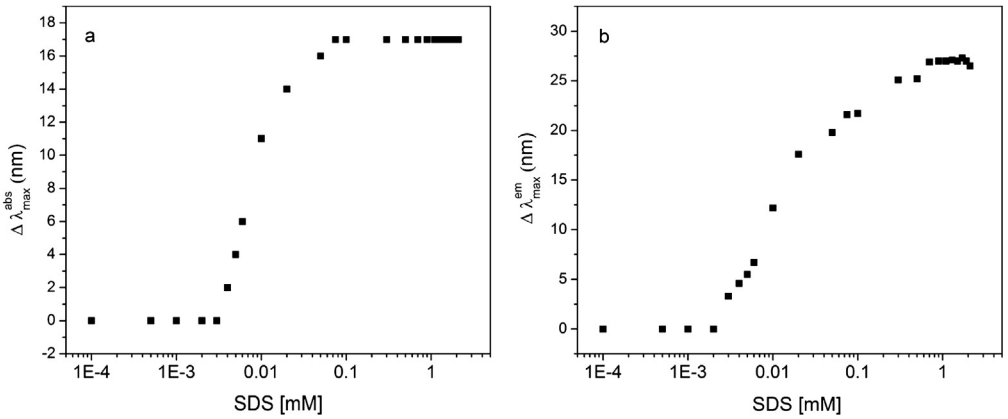

Fig. 4. Shifts of maximal absorption (a) and emission (b) bands of **1b** with increasing concentration of SDS.

the probe molecules, which induces the decrease of the microenvironment polarity.

Compounds **1a**, **1b** and **1c** have similar structures but different hydrophobic chain lengths. The changes of absorbance and fluorescence quantum yield of **1a** and **1c** are similar to those of **1b**, displaying "on–off–on" signal change, but the response concentration of **1a** is much higher, as shown in Fig. 5. As for **1c** with a longer chain, the response concentration is almost the same as **1b**, but the signal intensity is weaker. The increase of the hydrophobic chain length of probe leads to the decrease of solubility in water which is harmful for the application of probe. Therefore, for the purpose of detecting SDS, the length of the hydrophobic chain should be moderate.

To investigate the effects of the cationic headgroup on the sensing properties of these molecules, the photophysical properties of **1b**, **2b** and **3b** in the presence of SDS were investigated. The results are shown in Fig. 5. In the case of **3b**, the addition of SDS results in a similar change on the absorbance and fluorescence quantum yield with those of **1b** (on–off–on), but the response concentration is higher. The higher response concentration can be attributed to the large distance between N^+ and the N at C-4 position in **3b**, and then the bonding of SDS anion at N^+ leads to a relative weaker effect on the "push–pull" electronic configuration. In the case of **2b**, the change of absorbance is also similar with that of **1b**,

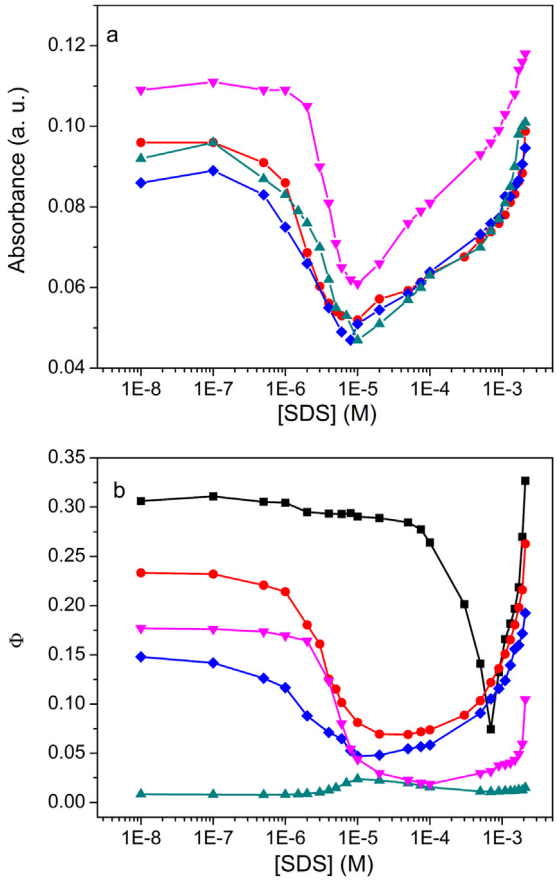

Fig. 5. Changes of absorbance (a) and fluorescence quantum yield (b) with increasing concentration of SDS. **1a** (■), **1b** (●), **1c** (♦), **2b** (▲) and **3b** (▼).

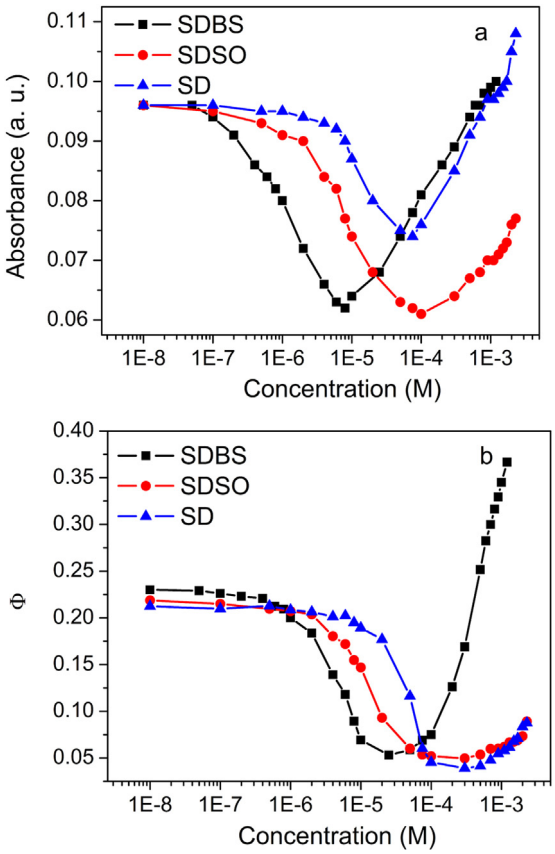

Fig. 6. Changes of absorbance (a) and fluorescence quantum yield (b) of **1b** with increasing concentration of SDBS (■), SDSO (●) and SD (▲).

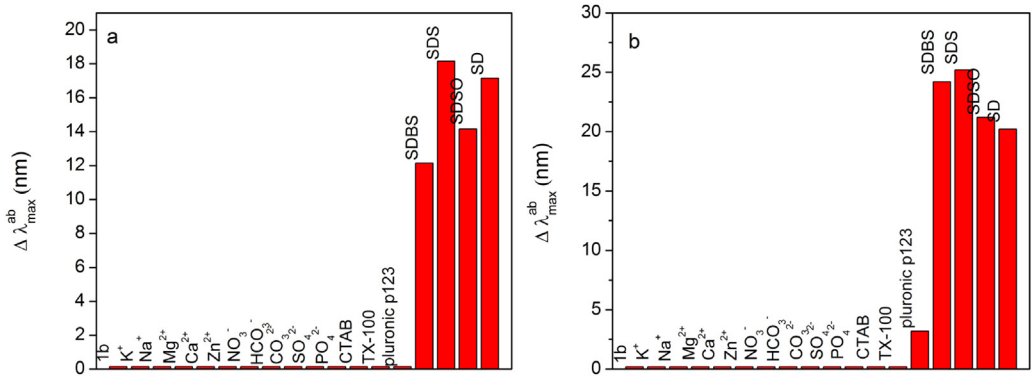

Fig. 7. Changes of the maximal absorption bands (a) and the maximal fluorescence bands (b) of **1b** in aqueous solution in the presence of various analytes. [**1b**] = 0.02 mM. [SDS] = [SDBS] = [SDSO] = [SD] = [CTAB] = 0.1 mM. [TX-100] = [p123] = 0.1 g/L. [simple ions] = 0.01 M.

however, the change of fluorescence quantum yield is opposite. Along with the increasing of SDS concentration, the fluorescence quantum yield of **2b** display "off–on–off" signal change and the signal intensity is pretty weak. This can be attributed to the different position of N^+ in **2b** and **1b** molecules and the contrary effects on the "push–pull" electronic configuration of these two molecules. Obviously, the position of N^+ and the distance between N^+ and N at C-4 position in probe molecule can affect the ability of probe.

3.4. Detection of other anionic surfactants by *1b*

As revealed by the experiments as mentioned above, **1b** is the best probe for detecting SDS in this group of compounds. The application of **1b** as probe for other anionic surfactants is also explored. Similar results were obtained with the addition of sodium dodecylbenzenesulfonate (SDBS), sodium dodecylsulfonate (SDSO), and sodium dodecanoate (SD) into the aqueous solution of **1b** (Fig. 6), indicating that **1b** is an efficient "on–off–on" fluorescence sensor for anionic surfactants. It is noted that the response concentrations of SDSO and SD are higher than those of SDS and SDBS. It is because sulfonate has a strong affinity for quaternary ammonium group with respect to carboxylate [11,31,32]. We can conclude that the stability of the complex formed between the molecule of anionic surfactant and probe is not only related to the structure of probe but also related to the anionic surfactant structure.

3.5. Selectivity toward anionic surfactants

To address the selectivity of **1b** toward anionic surfactants, absorption and fluorescence spectra of **1b** upon addition of hexadecyltrimethylammonium bromide (CTAB), Triton X-100 (TX-100), pluronic p123 and simple ions including K^+, Na^+, Mg^{2+}, Ca^{2+}, Zn^{2+}, NO_3^-, HCO_3^-, CO_3^{2-}, SO_4^{2-}, PO_4^{2-}, were examined under identical conditions. It was revealed that the maximal absorption band at 387 nm and the maximal fluorescence band at 525 nm changed distinctively only when anionic surfactants present. Only very small change on the maximal absorption and fluorescence bands can be identified in the presence of cationic, non-ionic surfactants and simple ions, Fig. 7. Moreover, most of the solutions remained light-yellow except for those containing anionic surfactants, which gave colorless solutions (Fig. S4). In the presence of cationic surfactants and nonionic surfactants, the absorption and emission intensity of **1b** solution increase slightly (Figs. S5 and S6), which are negligible in comparison with that induced by the anionic surfactants. It can be seen clearly in Fig. 8 that only anionic surfactants induced "on–off–on" changes in absorption and emission intensity (as shown in Fig. 2). Based on

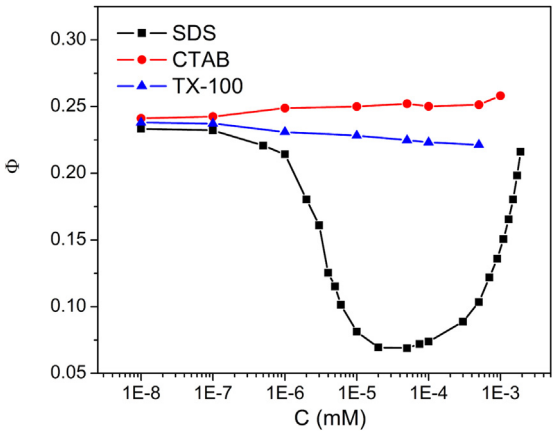

Fig. 8. Changes of fluorescence quantum yield of **1b** solution in the presence of various surfactants.

the results as mentioned above, we can conclude that the **1b** as a probe is highly selective toward anionic surfactants.

4. Conclusions

We have developed a series of colorimetric and fluorometric probes for detection of anionic surfactants in water based on cationic naphthalimide derivatives. Probe structure was demonstrated to be important in surfactant detection. Probe **1b** with proper hydrophobic chain length and cationic headgroup was confirmed to be the best choice for anionic surfactant detection in this series of compounds. The quantitative analysis of SDS can be realized in water and the detection low limit is around 1×10^{-7} M, which is almost equal to the standard methylene blue method [33], but the interference from the cationic and nonionic surfactants are avoided. We believe that the results demonstrated here will bring new inspiration in developing colorimetric sensing to anionic substrates in water.

Acknowledgements

We thank the Natural Science Foundation of China (Grant nos. 91233108 and 21173136), the National Basic Research Program of China (973 Program: 2012CB93280).

Appendix A. Supplementary data

Supplementary material related to this article can be found, in the online version, at http://dx.doi.org/10.1016/j.snb.2014.11.122.

References

[1] J.J. Scheibel, The evolution of anionic surfactant technology to meet the requirements of the laundry detergent industry, J. Surfactants Deterg. 7 (2004) 319–328.
[2] R. Pons, P. Taylor, T.F. Tadros, Investigation of the interactions in emulsions stabilized by a polymeric surfactant and its mixtures with an anionic surfactant, Colloid Polym. Sci. 275 (1997) 769–776.
[3] Y. Peng, Y. Hu, H. Wang, Tribological behaviors of surfactant-functionalized carbon nanotubes as lubricant additive in water, Tribol. Lett. 25 (2007) 247–253.
[4] Standard Methods for the Examination of Waters and Wastewaters, 19th ed., American Public Health Association, Baltimore, Maryland, 1995, pp. 5540.
[5] S.S.M. Hassan, I.H.A. Badr, H.S.M. Abd-Rabboh, Potentiometric flow injection analysis of anionic surfactants in industrial products and wastes, Microchim. Acta 144 (2004) 263–269.
[6] J.D.R. Thomas, Solvent polymeric membrane ion-selective electrodes, Anal. Chim. Acta 180 (1986) 289–297.
[7] A. Naader, K.-T. Hasan, Linear alkylbenzenesulfonate (LAS) ion-selective electrode based on electrochemically prepared polypyrrole and PVC, Sens. Actuators B 75 (2001) 5–10.
[8] B. Kovács, B. Csóka, G. Nagy, A. Ivaska, All-solid-state surfactant sensing electrode using conductive polymer as internal electric contact, Anal. Chim. Acta 437 (2001) 67–76.
[9] J. Sánchez, M. Valle, A new potentiometric photocurable membrane selective to anionic surfactants, Electroanalysis 13 (2001) 471–476.
[10] M.J. Seguí, J. Lizondo-Sabater, R. Martínez-Máñez, T. Pardo, F. Sancenón, J. Soto, Ion-selective electrodes for anionic surfactants using a new aza-oxa-cycloalkane as active ionophore, Anal. Chim. Acta 525 (2004) 83–90.
[11] Y. An, H. Bai, C. Li, G. Shi, Disassembly-driven colorimetric and fluorescent sensor for anionic surfactants in water based on a conjugated polyelectrolyte/dye complex, Soft Matter 7 (2011) 6873–6877.
[12] C. Coll, R. Casasús, E. Aznar, M.D. Marcos, R. Martínez-Máñez, F. Sancenón, J. Soto, P. Amorós, Nanoscopic hybrid systems with a polarity-controlled gate-like scaffolding for the colorimetric signalling of long-chain carboxylates, Chem. Commun. 19 (2007) 1957–1959.
[13] C. Coll, R. Martínez-Máñez, M.D. Marcos, F. Sancenón, J. Soto, A simple approach for the selective and sensitive colorimetric detection of anionic surfactants in water, Angew. Chem. Int. Ed. 46 (2007) 1675–1678.
[14] X. Chen, S. Kang, M.J. Kim, J. Kim, Y.S. Kim, H. Kim, B. Chi, S.-J. Kim, J.Y. Lee, J. Yoon, Thin-film formation of imidazolium-based conjugated polydiacetylenes and their application for sensing anionic surfactants, Angew. Chem. Int. Ed. 49 (2010) 1422–1425.
[15] J. Qian, X. Qian, Y. Xu, Selective and sensitive chromo- and fluorogenic dual detection of anionic surfactants in water based on a pair of on–off–on fluorescent sensors, Chem. Eur. J. 15 (2009) 319–323.
[16] Y. Zhao, X. Li, Aggregation behavior of naphthalimide fluorescent surfactants in aqueous solution, Colloid Polym. Sci. 292 (2014) 687–698.
[17] R.M. Duke, E.B. Veale, F.M. Pfeffer, P.E. Kruger, T. Gunnlaugsson, Colorimetric and fluorescent anion sensors: an overview of recent developments in the use of 1,8-naphthalimide-based chemosensors, Chem. Soc. Rev. 39 (2010) 3936–3953.
[18] H.S. Cao, D.I. Diaz, N.D. Cesare, J.R. Lakowicz, M.D. Heagy, Monoboronic acid sensor that displays anomalous fluorescence sensitivity to glucose, Org. Lett. 4 (2002) 1503–1505.
[19] D. Srikun, E.W. Miller, D.W. Domaille, C.J. Chang, An ICT-based approach to ratiometric fluorescence imaging of hydrogen peroxide produced in living cells, J. Am. Chem. Soc. 130 (2008) 4596–4597.
[20] D.F. Cauble, V. Lynch, M.J. Krische, Studies on the enantioselective catalysis of photochemically promoted transformations: sensitizing receptors as chiral catalysts, J. Org. Chem. 68 (2003) 15–21.
[21] D.W. Cho, M. Fujitsuka, A. Sugimoto, T. Majima, Intramolecular excimer formation and photoinduced electron-transfer process in bis-1,8-naphthalimide dyads depending on the linker length, J. Phys. Chem. A 112 (2008) 7208–7213.
[22] R. Ferreira, C. Baleizão, J.M. Muñoz-Molina, M.N. Berberan-Santos, U. Pischel, Photophysical sudy of bis(naphthalimide)-amine conjugates: toward molecular design of excimer emission switching, J. Phys. Chem. A 115 (2011) 1092–1099.
[23] J.X. Yang, X.L. Wang, X.M. Wang, L.H. Xu, The synthesis and spectral properties of novel 4-phenylacetylene-1,8-naphthalimide derivatives, Dyes Pigments 66 (2005) 83–87.
[24] R.F. Kubin, A.N. Fletcher, Fluorescence quantum yields of some rhodamine dyes, J. Lumin. 27 (1982) 455–462.
[25] K.H. Drexhage, Structure and properties of laser dyes, in: F.P. SchMer (Ed.), Dye Lasers, Topics in Applied Physics, 2nd ed, Springer, Berlin, 1977.
[26] J. Arden, G. Deltau, V. Huth, U. Kringel, D. Peros, K.H. Drexhage, Fluorescence and lasing properties of rhodamine dyes, J. Lumin. 352 (1991) 48–49.
[27] Y. Lin, X. Han, X. Cheng, J. Huang, D. Liang, C. Yu, pH-regulated molecular self-assemblies in a cationic-anionic surfactant system: from a 1–2 surfactant pair to a 1–1 surfactant pair, Langmuir 24 (2008) 13918–13924.
[28] K. Horbaschek, H. Hoffmann, J. Hao, Classic Lα phases as opposed to vesicle phases in cationic–anionic surfactant mixtures, J. Phys. Chem. B 104 (2000) 2781–2784.
[29] Y. Shen, Z. Ou-Yang, Y. Zhang, J. Hao, Z. Liu, Controlling the morphology of membranes by excess surface charge in cat-anionic fluorinated surfactant mixtures, Langmuir 30 (2014) 2632–2638.
[30] L. Xue, H. Wu, Y. Shi, H. Liu, Y. Chen, X. Li, Supramolecular organogels based on perylenetetracarboxylic diimide dimer or hexamer, Soft Matter 7 (2011) 6213–6221.
[31] Z. Yao, Y. Li, C. Li, G. Shi, Disassembly of conjugated polyelectrolyte aggregates and their application for colorimetric detection of surfactants in water, Chem. Commun. 46 (2010) 8639–8641.
[32] Z. Yao, H. Bai, C. Li, G. Shi, Analyte-induced aggregation of conjugated polyelectrolytes: role of the charged moieties and its sensing application, Chem. Commun. 46 (2010) 5094–5096.
[33] Water quality-determination of anionic surfactants-methylene blue spectrophotometric method, Chinese Government Standard GB-7494-37.

Biographies

Yingyuan Zhao graduated with Bachelor degree from Department of Chemistry of Shandong University in 2009. He received his Ph.D. in 2014 from Shandong University under the supervision of Prof. Xiyou Li. He is now a Research Scientist in the Research and Development Department of Shandong Matches Gramme Sis New Material Limited Company. His research interest includes new bioinorganic materials, supramolecular photochemistry, colloid and interface chemistry.

Xiyou Li got his Ph.D. from the Institute of Photographic Chemistry, Chinese Academy of Science in 1998. After that, he worked as a Humboldt Research Fellow in Bonn University (2001–2002), and Research Associate in Northwestern University (2002–2004). In 2004, he joined the Department of Chemistry of Shandong University as a full professor. In 2012, he was selected into the CAS "100 talents" program. His research interest includes Photophysics and Photochemistry, Photon–electron transfer, Photonic and Electronic Materials.